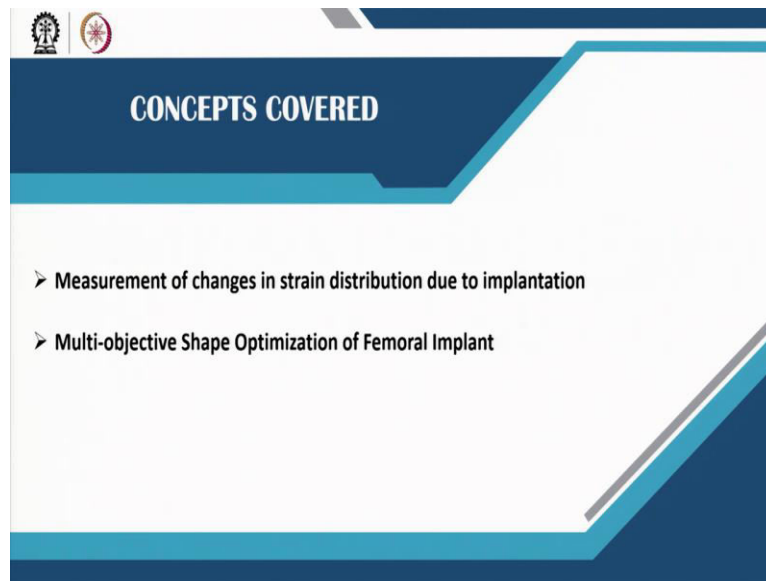


Biomechanics of Joints and Orthopaedic Implants
Professor. Sanjay Gupta
Department of Mechanical Engineering
Indian Institute of Technology, Kharagpur
Lecture 36
Design Optimization of HIP Implant

Good afternoon everybody. Welcome to the third lecture of module 7 on design optimization of HIP implant.

(Refer Slide Time: 0:41)



Now in this lecture, we will be discussing about experimental measurements regarding changes in strain distribution after hip implantation, which is a measure of strain shielding after implantation. Thereafter, we will be discussing about multi-objective shape optimization of femoral implant based on multi-objective shape optimization scheme.

(Refer Slide Time: 1:13)

Total Hip Replacement: A Background

- Average failure rate is approximately 10%, globally
- Mean duration before revision surgery is ~15–20 years
- ❑ The major causes of aseptic loosening and femoral fracture after THR are primarily due to biomechanical factors, sometimes governed by the design of implant.
- ❑ Demand for more durable implants are increasing
 - Young and active patients undergo replacements
 - Increase in life expectancy of older patients
 - More emphasis on customer specificity

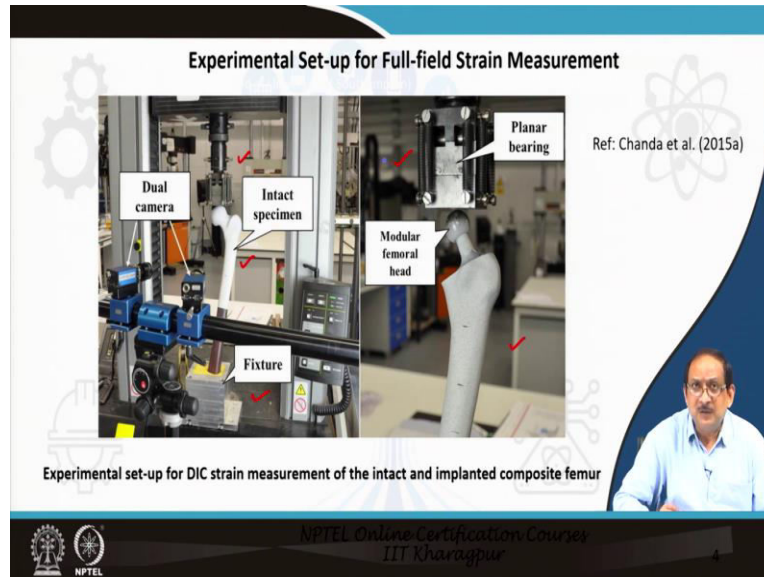
The slide features two radiographs: one on the left showing a hip with labels A, B, and C indicating areas of mechanical loosening, and one on the right showing a fractured stem labeled 'Broken stem'. A small inset image of a person is visible in the bottom right corner of the slide.

NPTEL Online Certification Courses
IIT Kharagpur

Total hip replacement is recognized as a successful reconstructive surgery for the treatment of hip joint disorders. However, the average failure rate is approximately 10 percent and the mean duration before revision surgery is around 15 to 20 years. The radiograph presented on the left presents a mechanically loose implant at locations A, B, and C whereas, the radiograph presented on the right presents a fractured implant.

The major causes of aseptic loosening and femoral fracture after total hip replacement, as recognized by the literature, are primarily due to biomechanical factors sometimes governed by the design of the implant. Now, the demand for more durable implants has been increasing, mainly because young and active patients undergo replacements, Increase in life expectancy of older patients, and more emphasis on customer specificity.

(Refer Slide Time: 2:58)

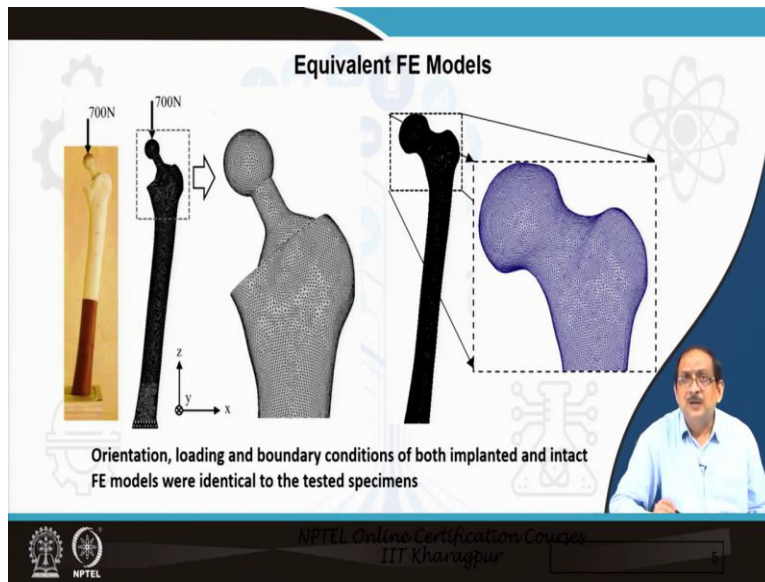


Now, this slide presents the experimental setup for full-field strain measurement in intact and implanted composite femurs using the digital image correlation technique. Now, here you can see in the figure presented in the slide that on the left, we have an intact specimen, and the specimen is fixed, maintaining the anatomic angles within a fixture; we have the dual cameras for recording the DIC measurements.

And the intact specimen, the composite femur has been painted with white paint on which black speckle patterns have been generated. On the right, we have an implanted femur using an uncemented furlong hip stem, and a similar procedure of painting it with white and followed by generation of speckle patterns have been employed for the DIC measurements.

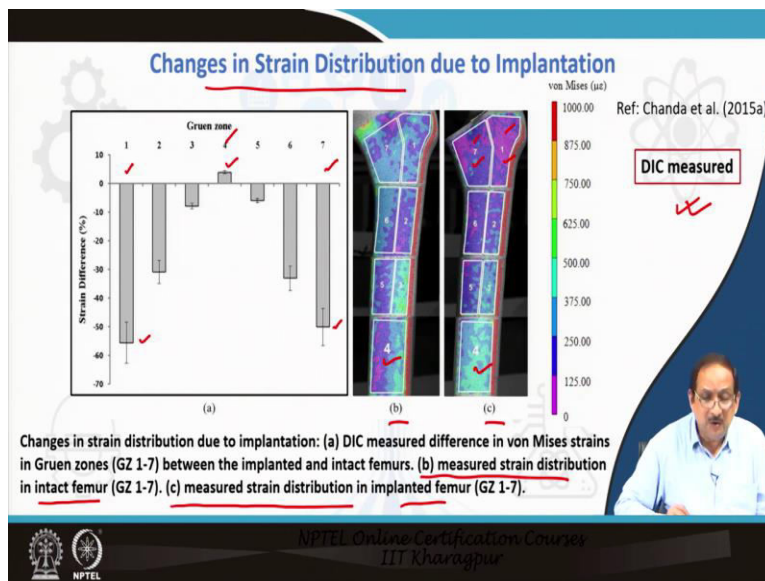
The loading mechanism discussed earlier has been used for the purpose of applying hip joint force on the index specimen as well as the implanted femur.

(Refer Slide Time: 4:53)



Thereafter we actually generated the equivalent finite element models mimicking the experiment. So, the orientation, loading and boundary conditions of both intact and implanted FE models were identical to the tested specimens.

(Refer Slide Time: 5:14)



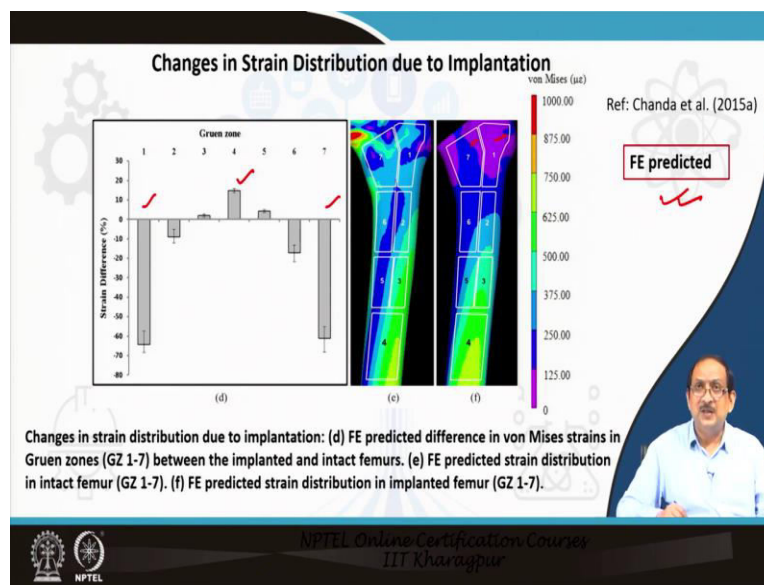
Let me now present to you the results regarding the changes in strain distribution due to implantation. In this slide, we are presenting the results on DIC measured strains. Figure B corresponds to the measured strain in the intact femur and figure C corresponds to the measured strain distribution in the implanted femur. Now, as you can see in the figure, that considerable

reductions in measured strains were observed in the lateral and medial cortex regions of the implanted femur represented by the Gruen zones 1 to 7.

Now, in the proximal part of the implanted femur, Gruen zone 1 recorded about 56 percent reduction in strain. And Gruen zone 7 recorded about 50 percent reduction in bone strains with standard deviation of ± 7 percent for both the cases. Now, on the figure on the left, you can see Gruen zone 1 experienced about 56 percent reduction in bone strain in the cortex and Gruen zone 7 experienced around 50 percent reduction in bone strains.

Now, as we move from the proximal towards the distal end, the effect of changes in bone strains after implantation was reduced. An increase in bone strain of 4 percent after implantation was measured in Gruen zone 4 around the distal tip of the implant.

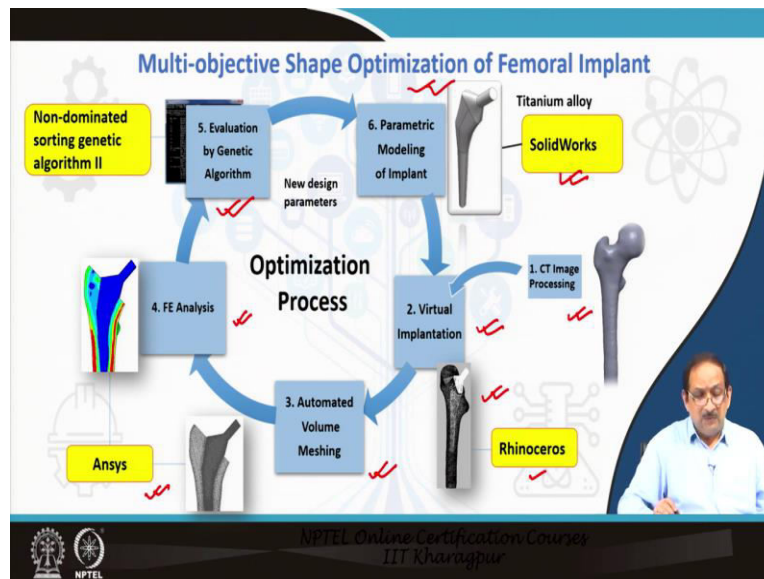
(Refer Slide Time: 7:41)



Now, similar trends were predicted by the FE analysis. The post-implantation strain shielding led to a reduction of strain of 60 percent in Gruen zone 1 and 7, but this reduction was consistent in most of the other Gruen zones and was closely related to clinically observed bone density changes around similar implants. Now, it can be seen from the load transfer patterns of the implanted femur that Gruen zone 1 and 7 experienced maximum strain shielding due to implantation and these other regions of maximum observed implant induced long term bone resorption clinically.

Proximal bone density loss corresponded to 50 to 64 percent reduction in the bone strains, whereas distal bone density gain corresponded to 4 to 14 percent increase in the bone surface strains.

(Refer Slide Time: 9:22)



Now, let us move into the second topic on multi-objective shape optimization of the femoral implant. As you already know that the adverse effects of implant-induced bone resorption and excessive interface stresses have often been reported as potential causes of failure in cementless total hip arthroplasty or total hip replacement. The shape of the implant influences both these failure mechanisms. These failure mechanisms may be mutually conflicting in nature.

A bone preserving stem may reduce adverse bone resorption considerably but increase the chances of interface failure due to excessive stresses. Hence, employing shape optimization scheme stem designs were evaluated based on these two major failure mechanisms. Now, as you can see here in the figure that the starting point is the CT scan image, so, after image processing, we can actually generate the solid model.

And perform the virtual implantation may be using specific software. In our case, we had used rhinoceros. Thereafter, we do the mesh generation using automated volume meshing. Within FE software Ansys and after applying the musculoskeletal loading conditions, we can actually perform the finite element analysis. After the finite element analysis, the optimization controller,

in this case, the non-dominated sorting genetic algorithm 2, commonly known as NSGA 2, is actually used for evaluating the design of the design variables.

The optimization controller initialized new values for the design variables. These design variables are fed to the CAD package in order to generate new implant geometry. Thereafter, the new implant model is virtually implanted into the resected femur model. The STL file of the implanted femur can be meshed using the automatic mesh generator. And finally, we can perform the finite element analysis.

So, a program written in Ansys parametric design language served as the FE analysis script and the analysis results were used by MATLAB script to calculate the objective functions. These values of the objective functions were fed to the optimization controller for strategizing a set of design variables and the cycle was repeated. All procedures were integrated and automated through scripts so that the whole computational scheme could run in an unattended mode.

Once the optimized implant geometries were obtained, bone remodeling simulations were carried out in order to assess the long-term periprosthetic bone remodeling and its further influence on implant-bone interface failure. We now move on to the details of the optimization procedure.

(Refer Slide Time: 13:53)

Shape Optimization: Parameterization

- The initial design of the stem was similar to a generic design of a collarless TriLock (DePuy) prosthesis having stem-length 113 mm, which was kept unaltered.
- Four key sections of the hip stem were considered for the shape optimization procedure.

$x = a \cdot \cos^{(2/p)} t$
 $y = b \cdot \sin^{(2/p)} t$

Eighteen (18) design parameters were introduced
 Limits of t were prescribed as $0 \leq t \leq \pi/2$

Ref: Chanda et al. (2015b)

The slide includes a 3D model of a hip stem, a 2D cross-section with parameters a , b , and t , and a series of cross-sections labeled aa , bb , cc , and dd corresponding to different sections of the stem. A small inset shows a graph of the parametric equations.

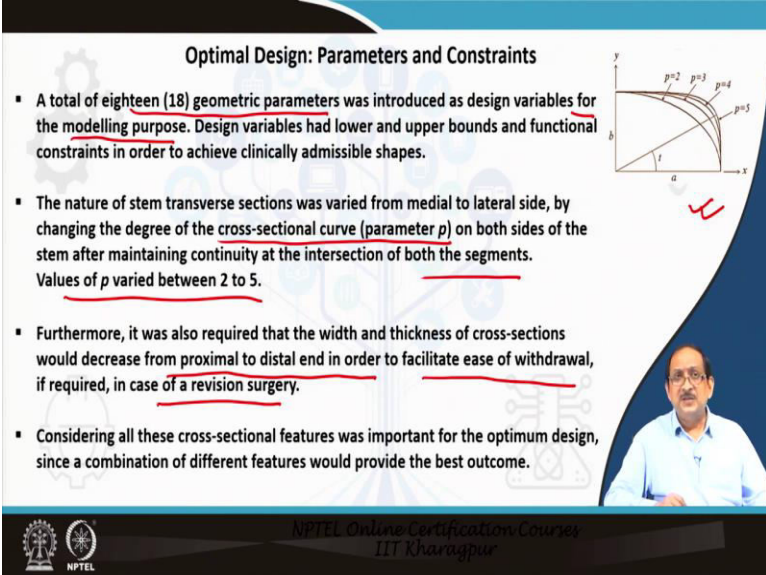
And let us now introduce the parameterization in the shape optimization scheme. The initial design of the hip stem was based on a generic design of a collarless TriLock hip stem having a stem length of 113 millimeter. The stem length was kept unaltered throughout the analysis. Now,

4 key sections of the hips stem A, B, C, D, as indicated in the figure here, were considered for the shape optimization procedure.

Now, in each of these key sections, the local coordinate system x and y is defined. And a pair of equations that define the geometric parameterization of the stem transverse section was expressed in parametric form, as indicated here in the slide. Here, the limits of the t were prescribed in the range of 0 and $\pi/2$. Whereas the parameters A , B , and P at 4 key sections characterized the design parameters of the femoral stem.

The nature of stem transfer sections was varied by changing the degree of cross-sectional curves, the parameter P , which varied from 2 to 5.

(Refer Slide Time: 16:00)



Optimal Design: Parameters and Constraints

- A total of eighteen (18) geometric parameters was introduced as design variables for the modelling purpose. Design variables had lower and upper bounds and functional constraints in order to achieve clinically admissible shapes.
- The nature of stem transverse sections was varied from medial to lateral side, by changing the degree of the cross-sectional curve (parameter p) on both sides of the stem after maintaining continuity at the intersection of both the segments. Values of p varied between 2 to 5.
- Furthermore, it was also required that the width and thickness of cross-sections would decrease from proximal to distal end in order to facilitate ease of withdrawal, if required, in case of a revision surgery.
- Considering all these cross-sectional features was important for the optimum design, since a combination of different features would provide the best outcome.

The diagram shows a coordinate system with x and y axes. A curve is plotted in the first quadrant, starting at the origin and ending at a point (a, b) . The curve is defined by the parameter p , with values $p=2, p=3, p=4, p=5$ shown. A red checkmark is visible next to the diagram.

NPTEL Online Certification Courses
IIT Kharagpur

A total number of 18 geometric parameters was introduced as design variables for the modeling purpose. Designed variables had lower and upper bounds and functional constraints in order to achieve clinically admissible shapes. The nature of stem transfer sections was varied from medial to lateral side by changing the degree of the cross-sectional curve, that is, the parameter p on both sides of the stem after maintaining continuity at the intersection of both the segments.

The values of p varied between 2 to 5, as you can see here in the figure presented in the slide. Furthermore, it was also required that the weight and thickness of cross-sections would decrease from the proximal to the distal end in order to facilitate ease of withdrawal if required in case of revision surgery. Considering all these cross-sectional features was important for the optimum

design since a combination of different features would provide the best outcome.

(Refer Slide Time: 17:34)

$x = a \cos^{(2/p)} t$
 $y = b \sin^{(2/p)} t$

Design Variables

- The parameters:
 - $a1 - a6$: length of major axes on medial and lateral sides
 - $b1 - b4$: length of the minor axes.
- Degree of the curve segments (values of p) on the:
 - medial side: designated as $p1, p3, p5$ and $p7$
 - lateral side: designated as $p2, p4, p6$ and $p8$

NPTEL Online Certification Courses
IIT Kharagpur

So, the design parameter meters can be summarized here. $a1$ to $a6$: the six parameters are the length of the major axis on medial and lateral sites. $b1$ to $b4$ are the lengths of the minor axis as indicated in the figure as well. The degree of the curve segments that is the value of p on the medial side designated as $p1, p3, p5, p7$ and on the lateral side is designated as $p2, p4, p6$ and $p8$ as indicated in the figure here in the slide.

(Refer Slide Time: 18:24)

Fully Automated Shape Optimization Framework

- Geometric parameters were introduced to characterize the femoral stem shape.
- Objective functions were formulated based on two common failure mechanisms of uncemented Total Hip Replacement.
- This optimization scheme comprises of a parametric implant model generator, a script for virtual implantation, an automatic mesh generator, an FE analysis script and finally, an optimization controller. In order to integrate all these components, a master program was developed.
- A multi-objective GA is used to strategize design variables for a new implant model and subsequently, the master program was launched to evaluate the design.

Goal of the Optimization was to Minimize: Stress-shielding and proximal bone resorption and implant-bone interface stresses

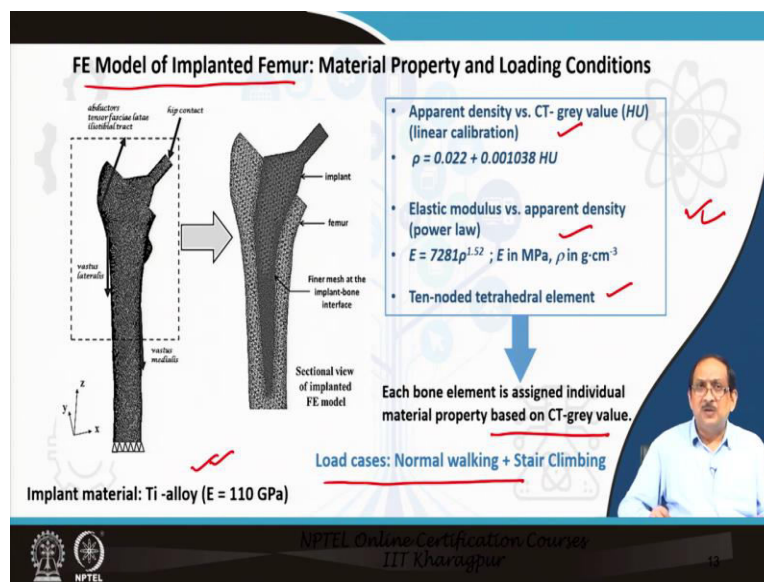
NPTEL Online Certification Courses
IIT Kharagpur

Now, this is a fully automated shape optimization framework. So, geometric parameters were introduced to characterize the femoral stem shape. The objective functions of the optimization

framework were formulated based on two major common failure mechanisms of the cementless total hip replacement. This optimization scheme comprises of a parametric implant model generator, a script for virtual implantation, an automatic mesh generator, an FE analysis script, and finally, an optimization controller.

In order to integrate all these components, a master program was developed. A multi-objective genetic algorithm is used to strategize design variables of a new implant model and subsequently, the master program was launched to evaluate the design. The goal of the optimization scheme was to minimize stress shielding and proximal bone resorption and implant-bone interface stresses.

(Refer Slide Time: 19:58)



So, we developed the FE model of the implanted femur with the trilock hip stem and the implanted model was based on CT scan data of a subject. So, here you can see the generation procedure has been summarized. So, from CT scan image processing, we generate the solid model and then the finite element mesh and we allocate bone material properties to individual bone elements in the finite element model based on the CT gray value, the linear calibration and the power law relationship between elastic modulus and apparent density.

So, we used ten noded tetrahedral elements. The loading conditions included the activities of normal walking and stair climbing and the implant material is titanium alloy with Young's modulus of 110 Giga Pascal.

(Refer Slide Time: 21:42)

Objective Function Formulation and Design Goal

Minimize Objective Function 1:

Stress shielding $f1 = \frac{1}{M} \int_V K(U, \rho) \rho dV$

where M (g) and V (cm^3) represent the total mass and volume of the implanted proximal femur, respectively.

Minimize Objective Function 2:

Interface stresses $f2 = \frac{1}{\Pi} \int_{\Pi} \{FL\}^m d\Pi$

where Π is total implant-bone interfacial area, $m = 2$ is the attenuation parameter.

subject to constraints:

$a_2 - a_1 \geq 0; b_2 - b_1 \geq 0; a_4 - a_2 \geq 0; b_3 - b_2 \geq 0; a_5 - a_4 \geq 0; b_4 - b_3 \geq 0;$
 $a_3 - a_2 - 4.5 \geq 0; a_5 - a_3 - 4.5 \geq 0; a_5 - a_3 - 7.0 \leq 0; a_2 + a_5 - 2.0 \times a_3 \geq 0;$

Resorbed Bone Mass Fraction

Hoffman Failure Criterion

$K(U, \rho) = \begin{cases} 1, & \text{if } S \leq (1-s)S_{off} \\ 0, & \text{otherwise} \end{cases}$

Ref: Chanda et al. (2015b)

Now comes the most important slide of the lecture; the formulation of the objective functions. The goal of the optimization procedure was to minimize both the objective functions subject to the functional constraints. Unlike an optimum solution obtained in the case of single objective optimization procedure, multi-objective optimization provides a set of solutions. Now, let me now explain objective function 1, which is based on stress shielding and related to the resorbed bone mass fraction.

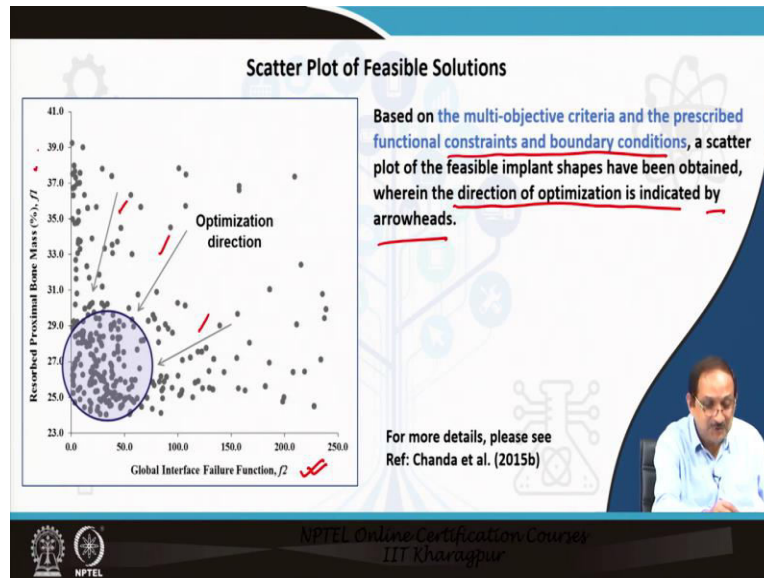
Now, we need to minimize stress shielding by minimizing resorbed bone mass fraction, as indicated here in the slide. Now, since bone resorption predominantly occurs in the proximal part of the femur. The calculations of bone mass fraction were confined to the bone elements located in the proximal femur, both intact and implanted up to the lesser trochanter.

The calculation of the bone mass fraction was based on the adaptive bone remodeling theory. And according to this theory, the change in bone density is dependent on the difference in mechanical stimulus between the intact and the implanted bone. We next come to the objective function to which is based on the interface stresses. Now, the interface stress evaluation is in turn based on the multiaxial Hoffmann failure criteria.

So, it is the Hoffman failure criteria that actually indicates the chances of local interface failure within the implant-bone structure. And our objective was to minimize both the objective

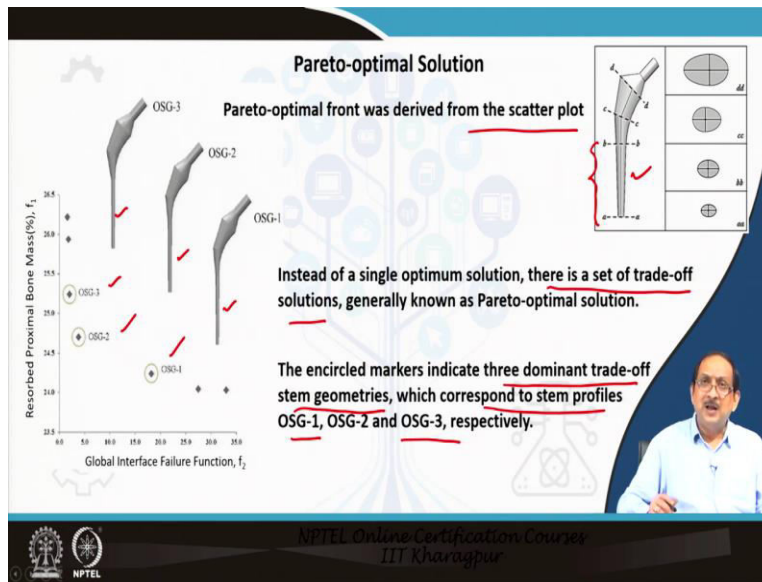
functions subject to the functional constraints or geometric constraints as indicated here in the slide.

(Refer Slide Time: 24:37)



Now, based on the multi-objective criteria and the prescribed functional constraints and the boundary conditions, a scatter plot of the feasible implant shapes has been obtained wherein the direction of optimization is indicated by the arrowheads. Now, it is evident from the figure that the two objective functions were conflicting in nature; the global interface failure function F_2 and the resorbed proximal bone mass F_1 .

(Refer Slide Time: 25:23)

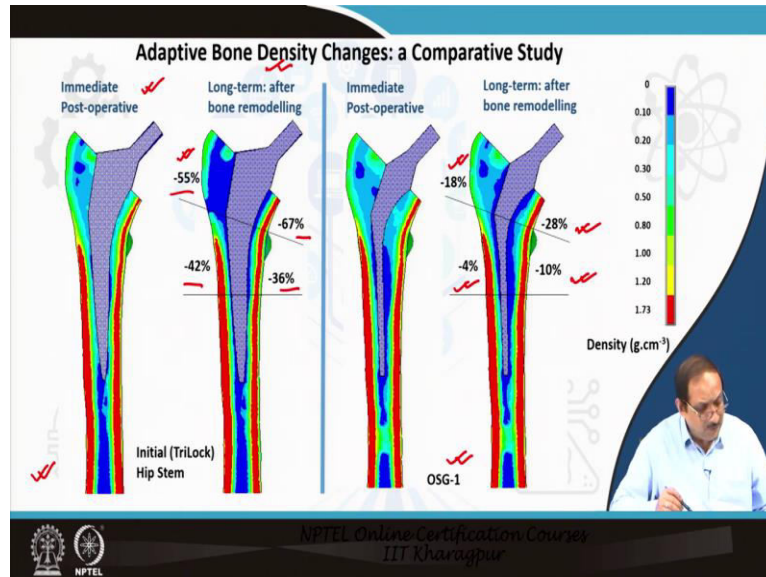


Within this set of solutions, the Pareto optimal front solutions are obtained and three dominant trade-off geometries were chosen as optimal stem geometries OSG 1 2 and OSG3 for detail analysis. Now, Pareto optimal front was derived from the scatter plot. Instead of a single optimum solution, there is a set of trade of solutions generally known as the Pareto optimal solution. The encircled markers indicate the three dominant trade-off stem geometries, which correspond to stem profiles OSG 1, 2, and 3, respectively.

These implant shapes were found to be minimally invasive as compared to the initial implant that is the trilock hip stem. It should be clarified here that the term minimally invasive stem implies stem geometries have dimensions smaller than the standard hip stem. It is also worth noting in this figure the emergence of narrow distal parts between the sections a to b.

So, the emergence of the narrow distal parts in all the optimal designs suggests that there is hardly any requirement of the long distal stem for the purpose of load transfer provided sufficient bone ingrowth occurred into the porous coating of the implant. Therefore, a long stem as compared to a short one may be useful for facilitating bone ingrowth and for distal fixation.

(Refer Slide Time: 27:52)

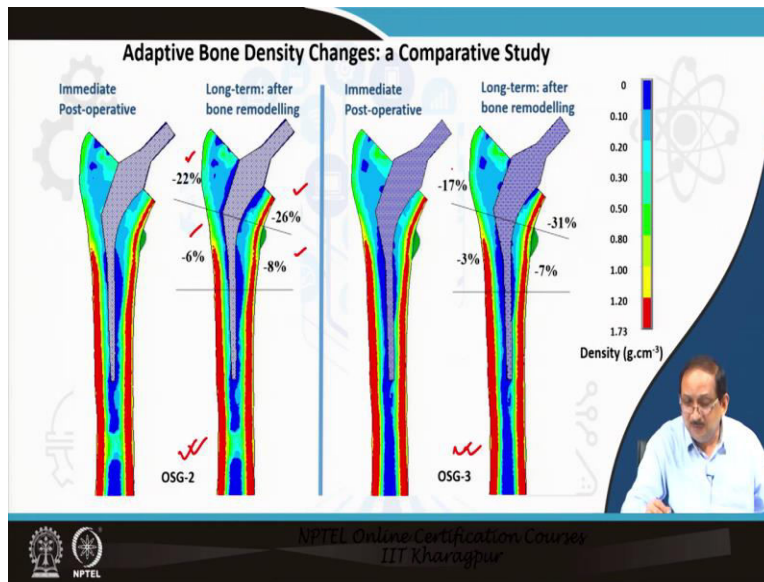


Let us now come to the adaptive bone density changes and comparison between the initial hip stem, the trilock stem, and later the effects of optimized stem geometries 1, 2, and 3 on the adaptive bone density changes. So, on the left, we first present the immediate post-operative bone density configuration. Now, long-term bone remodeling is indicated here; the negative sign indicates bone resorption.

So, you can see on the proximal part of the implanted femur; there is a considerable amount of adverse bone remodeling in the form of bone resorption. So, -55 % of bone density reduction, -67 % bone density reduction, -42 % and -36 %; this corresponds to the initial trilock of hips stem.

Thereafter, when we investigate the bone density changes with optimal stem geometry 1, these percentages of bone resorption or bone density reductions reduces to -18 %, -28 %, -4 %, and -10 % as compared to the figure on the left for the trilock hip stem.

(Refer Slide Time: 29:49)



Similar, bone density changes were actually obtained for optimized geometry 2 and 3 as you can see here - 22 %, - 26 %, - 6 % and - 8 %; remember negative sign denotes bone resorption, that is decreased or reduction in bone density. In case of optimal stem geometry – 3 %, - 17 %, - 31 %, and - 7 %.

(Refer Slide Time: 30:27)

CONCLUSION

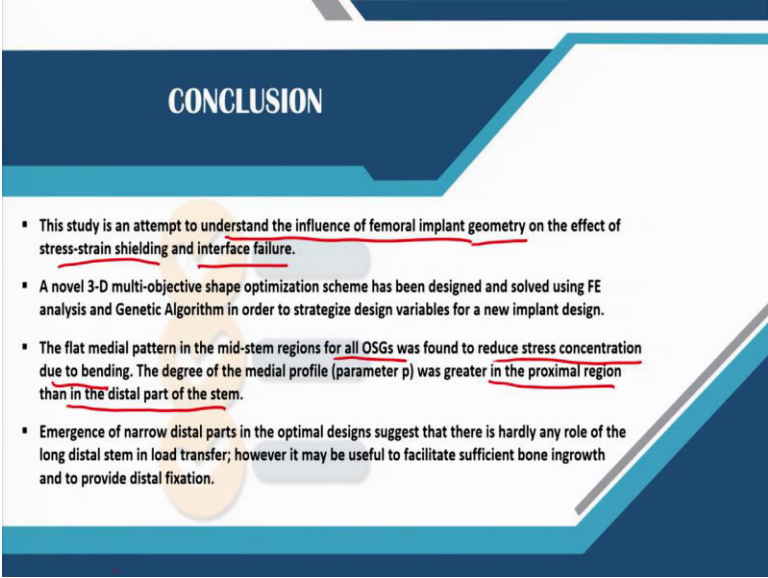
- This study is an attempt to understand the influence of femoral implant geometry on the effect of stress-strain shielding and interface failure.
- A novel 3-D multi-objective shape optimization scheme has been designed and solved using FE analysis and Genetic Algorithm in order to strategize design variables for a new implant design.
- The flat medial pattern in the mid-stem regions for all OSGs was found to reduce stress concentration due to bending. The degree of the medial profile (parameter p) was greater in the proximal region than in the distal part of the stem.
- Emergence of narrow distal parts in the optimal designs suggest that there is hardly any role of the long distal stem in load transfer; however it may be useful to facilitate sufficient bone ingrowth and to provide distal fixation.

Let us now come to the conclusions of this study. So, this study is an attempt to understand the influence of femoral implant geometry on the effect of stress-strain shielding and interface failure. A novel three-dimensional multi-objective shape optimization scheme has been

developed and solved using finite element analysis and genetic algorithm in order to strategize design variables for a new implant design.

The flat medial pattern in the mid stem regions for all optimal stem geometries was found to reduce stress concentration due to bending. The degree of the medial profile that is parameter p was greater in the proximal region than in the distal part of the stem. Emergence of narrow distal parts in the optimal designs suggests that there is hardly any role of the long distal stem in load transfer. However, it may be useful to facilitate sufficient bone ingrowth and to provide distal fixation.

(Refer Slide Time: 31:57)



CONCLUSION

- This study is an attempt to understand the influence of femoral implant geometry on the effect of stress-strain shielding and interface failure.
- A novel 3-D multi-objective shape optimization scheme has been designed and solved using FE analysis and Genetic Algorithm in order to strategize design variables for a new implant design.
- The flat medial pattern in the mid-stem regions for all OSGs was found to reduce stress concentration due to bending. The degree of the medial profile (parameter p) was greater in the proximal region than in the distal part of the stem.
- Emergence of narrow distal parts in the optimal designs suggest that there is hardly any role of the long distal stem in load transfer; however it may be useful to facilitate sufficient bone ingrowth and to provide distal fixation.

The list of references, though very short here because it is based on basically two studies by our group, has been presented here, and I thank you for listening.